

## Novel Guest-Layer Behavior of Mercury Titanium Disulfide Intercalates

Max V. Sidorov,<sup>†,‡</sup> Michael J. McKelvy,<sup>\*,†,‡</sup>  
John M. Cowley,<sup>§</sup> and William S. Glaunsinger<sup>†,‡,||</sup>

Center for Solid State Science, Science and Engineering of Materials Graduate Program, Department of Physics and Astronomy, and Department of Chemistry and Biochemistry, Arizona State University, Tempe, Arizona 85287-1704

Received June 19, 1998

Revised Manuscript Received August 11, 1998

One of the most widely studied classes of intercalation compounds are the metal intercalates of the transition-metal disulfides.<sup>1,2</sup> These materials can be generally described as ionic compounds, with their ionic guests typically occupying individual sites between the host lamella. Intriguing exceptions to this broad range of materials are the mercury intercalates.<sup>3–12</sup> Unlike other metal guests, Hg is essentially neutral and exhibits very weak guest–host electron exchange. The unique nature of Hg contributes to the unusual properties of these intercalates, including thermally reversible intercalation, superstoichiometric mercury uptake (e.g.,  $\text{Hg}_x\text{TiS}_2$ ,  $1.24 \geq x \geq 0.00$ ), and formation of infinite mercury chains that are incommensurate with the host structure, as shown in Figure 1.<sup>9,11</sup>  $\text{Hg}_x\text{TiS}_2$  has a novel (3 + 1) dimensional structure,<sup>10,11</sup> described by interpenetrating  $\text{TiS}_2$  and Hg monoclinic sublattices, with common  $a$  and  $c$  axes and incommensurate  $b$  axes parallel to the Hg chains.

In the fully intercalated compound,  $\text{Hg}_{1.24}\text{TiS}_2$ , the host-layer channels, in which the Hg chains reside, provide trigonal prismatic (TP) coordination [ $\beta = 102^\circ$  structural modification;  $a = 5.92 \text{ \AA}$ ,  $b(\text{TiS}_2) = 3.41 \text{ \AA}$ ,  $b(\text{Hg}) = 2.76 \text{ \AA}$ ,  $c = 8.86 \text{ \AA}$ , and  $\beta = 102.3^\circ$ ]. Early in

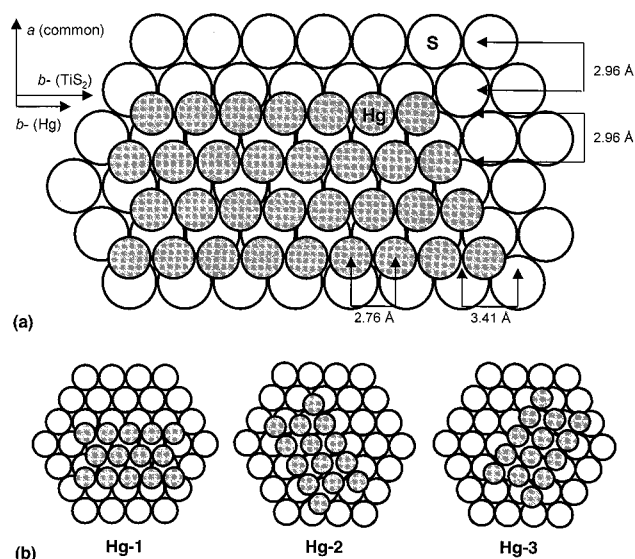


**Figure 1.** (a) A model of the in-plane structure of  $\text{Hg}_x\text{TiS}_2$  viewed perpendicular to the layers showing the formation of partially commensurate Hg guest layers for a single Hg sublattice orientation. The Hg layers are composed of infinite chains of atoms aligned along the incommensurate  $b$  direction midway between neighboring sulfur rows. (b) A model showing the three equivalent orientational variants of Hg with respect to the host layers.

the deintercalation process, minimization of host-layer elastic strain induces a  $1/2b$  host-layer shift along the Hg chains, resulting in distorted trigonal antiprismatic (DTAP) coordination of the intercalate galleries and the  $\beta = 96^\circ$  structural modification [ $\text{Hg}_x\text{TiS}_2$  ( $x < 1.24$ );  $a = 5.92 \text{ \AA}$ ,  $b(\text{TiS}_2) = 3.41 \text{ \AA}$ ,  $b(\text{Hg}) = 2.76 \text{ \AA}$ , and  $\beta = 96.5^\circ$ ].<sup>10,11</sup> The structure of the Hg-chain guest layers is little affected by deintercalation.

The novel one-dimensional nature of the guest layers has motivated study of their behavior as a function of temperature to better understand the guest–guest and guest–host interactions in this new class of metal-intercalated transition-metal disulfide intercalation compounds. X-ray powder diffraction (XPD) and differential scanning calorimetry (DSC) studies of the fully intercalated  $\beta = 102^\circ$  phase indicate that the Hg chains undergo a guest-layer melting transition near  $200^\circ\text{C}$ ,<sup>5,12</sup> after which only the  $00l$  reflections and the reflections uniquely associated with the host lattice remain. Herein, we follow the temperature-dependent behavior of the  $\beta = 96^\circ$  phase by electron diffraction, prior to and during deintercalation, by combining sample-stage temperature control ( $\geq -170^\circ\text{C}$ ) with electron-beam heating. The phase is well-ordered at low temperatures, develops increasing interchain disorder with increasing temperature, and eventually undergoes an intriguing partial-melting transition at higher temperatures.

The initial material used for these in situ studies, stage-1  $\text{Hg}_{1.24}\text{TiS}_2$ , was prepared by direct reaction of stoichiometric amounts of high-purity Hg (<5 ppm metal impurities) and  $\text{TiS}_2$  at  $320^\circ\text{C}$ , followed by slow cooling to ambient temperature.<sup>3–5</sup> The host, highly stoichiometric  $\text{TiS}_2$  ( $\text{Ti}_{1.002}\text{S}_2$ ), was prepared by direct reaction of the elements. The  $\text{TiS}_2$  was compositionally

<sup>†</sup> Center for Solid State Science.

<sup>‡</sup> Science and Engineering of Materials Graduate Program.

<sup>§</sup> Department of Physics and Astronomy.

<sup>||</sup> Department of Chemistry and Biochemistry.

(1) Lévy, F., Ed. *Intercalated Layered Materials*; D. Reidel: Dordrecht, Holland, 1979.

(2) Whittingham, M. S.; Jacobson, A. J., Eds. *Intercalation Chemistry*; Academic Press: New York, 1982.

(3) Ong, E. W., Ph.D. Thesis, Arizona State University, Tempe, Arizona, 1990.

(4) McKelvy, M.; Sharma, R.; Ong, E.; Burr, G.; Glaunsinger, W. *Chem. Mater.* **1991**, *3*, 783.

(5) Ong, E. W.; McKelvy, M. J.; Ouvrard, G.; Glaunsinger, W. S. *Chem. Mater.* **1992**, *4*, 14.

(6) Moreau, P.; Ouvrard, G. *Chemical Physics of Intercalation II*; Bernier, P., Fischer, J. E., Roth, S., Solin, S. A., Eds.; NATO ASI Series Vol. 305, Plenum Press: New York, 1993; p 351.

(7) Ganal, P.; Olberding, W.; Butz, T.; Ouvrard, G. *Chemical Physics of Intercalation II*; Bernier, P., Fischer, J. E., Roth, S., Solin, S. A., Eds.; NATO ASI Series Vol. 305, Plenum Press: New York, 1993; p 383.

(8) Moreau, P.; Ganal, P.; Ouvrard, G. *Mol. Cryst. Liq. Cryst.* **1994**, *244*, 325.

(9) McKelvy, M.; Sidorov, M.; Marie, A.; Sharma, R.; Glaunsinger, W. *Chem. Mater.* **1994**, *6*, 2233.

(10) Ganal, P.; Moreau, P.; Ouvrard, G.; Sidorov, M.; McKelvy, M.; Glaunsinger, W. *Chem. Mater.* **1995**, *7*, 1132.

(11) Sidorov, M.; McKelvy, M.; Sharma, R.; Glaunsinger, W.; Ganal, P.; Moreau, P.; Ouvrard, G. *Chem. Mater.* **1995**, *7*, 1140.

(12) Moreau, P.; Ganal, P.; Lemaux, S.; Ouvrard, G.; McKelvy, M. *J. Phys. Chem. Solids* **1996**, *57*, 1129.

and structurally characterized by oxidative thermogravimetric analysis (TGA) and XPD, respectively.<sup>13,14</sup> The initial intercalate composition ( $\text{Hg}_{1.24 \pm 0.01}\text{TiS}_2$ ) was determined by TGA of the complete deintercalation process under flowing argon.<sup>5</sup>

HRTEM samples were prepared by crushing the intercalate at  $-196^\circ\text{C}$  in a nitrogen-containing glovebox, warming the freshly crushed crystallites to ambient temperature and dispersing them on holey carbon-coated copper TEM grids. XPD and TGA compositional analyses confirmed that no significant structural or compositional change occurred during sample preparation.<sup>4,5,9</sup>

The electron diffraction investigations were performed using a JEOL 2000FX electron microscope equipped with a special Gatan variable-temperature ( $-170^\circ\text{C}$  to  $150^\circ\text{C}$ ) inert-atmosphere transfer holder. Samples were loaded into the holder in the glovebox, cooled to  $-170^\circ\text{C}$ , and inserted into the microscope. Initial observations at  $-170^\circ\text{C}$  showed some deintercalation of the samples had occurred, which induces the  $102^\circ$  to  $96^\circ$  phase transition.<sup>11</sup> The initially observed deintercalation is probably associated with the temperature gradient that develops between the sample grid and the sample during cooldown. Electron diffraction was then used to follow the structural behavior of the Hg guest layers as a function of increasing temperature and degree of deintercalation via combined sample-stage and electron-beam heating.

The basic in-plane structure of the ambient temperature  $\beta = 96^\circ$  phase is shown, together with the three equivalent orientational variants of the guest-layer structure, in Figure 1. Figure 2 shows schematic representations of the electron diffraction patterns that arise from the four different sublattice components (the  $\text{TiS}_2$  sublattice and the three variants of the Hg sublattice) and a crystal containing significant amounts of each sublattice component.<sup>11</sup> Each Hg-sublattice variant is equivalent to the other two when rotated by  $\pm 120^\circ$  about an axis perpendicular to the layers. The variants differ only in the direction of the Hg chains and the DTAP host-layer channels that house them. Thicker crystals were found to contain essentially equivalent amounts of each orientational variant, while very thin crystals contained primarily one variant. This indicates a small number of galleries containing a single variant tend to group together, a possible consequence of lamellar nucleation and growth processes during intercalation.<sup>11</sup>

To provide enough diffraction intensity to follow the in-plane Hg structure as a function of temperature and deintercalation level, relatively thick crystals containing all three orientational variants were observed perpendicular to the layers. Representative electron diffraction patterns from a single  $\text{Hg}_x\text{TiS}_2$  crystal as a function of increasing temperature and deintercalation level are shown in Figure 3. The crystal contains similar amounts of the three orientational variants, as indicated by the similar intensity of the Hg sublattice reflections.<sup>11</sup> The initial pattern at a substrate temperature of  $-170^\circ\text{C}$

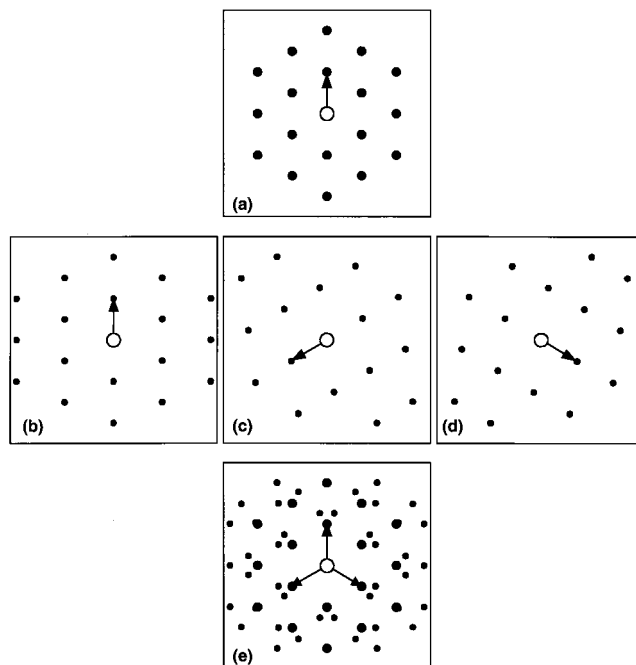


**Figure 2.** A schematic depiction of the electron diffraction patterns that arise from (a) the  $\text{TiS}_2$  sublattice, (b–d) the three orientational variants (Hg-1, Hg-2, and Hg-3) of the Hg sublattice, and (e)  $\text{Hg}_x\text{TiS}_2$ . The  $a^*$  axes and 200 reflections (at the end of each arrow) are indicated for each sublattice.

is shown in Figure 3a, together with a schematic depiction of the pattern identifying the primary  $\text{Hg}_x\text{TiS}_2$  reflections and those arising from double diffraction overlaying the pattern on the left. Of particular interest is the well-defined crystalline order of both the Hg and  $\text{TiS}_2$  sublattice reflections, indicating that both sublattices are well-ordered at low temperature. This is highlighted by the observation of extensive double diffraction. Figures 3b–d show the diffraction pattern from the same crystal taken at progressively higher substrate temperatures up to  $50^\circ\text{C}$ , with similar levels of electron-beam heating. The diffraction spots arising from double diffraction are rapidly lost on heating, suggesting increasing disorder. Diffuse streaks also develop along the  $a^*$  direction for the  $(hk0, k \neq 0)$  Hg sublattice reflections, suggesting that correlated atomic displacements of the Hg chains are temperature-induced (along  $b$ ). Continued heating to  $50^\circ\text{C}$  further induces deintercalation and gives rise to the pattern shown in Figure 3d. As expected, the primary reflections are associated with the deintercalated regions of the crystal with the  $\text{TiS}_2$  in-plane structure. However, in addition to weak reflections associated with residual intercalated regions containing the three  $\text{Hg}_x\text{TiS}_2$  orientational variants, a weak new diffraction ring containing faint spots arises with a spacing of  $2.70 \pm 0.03 \text{ \AA}$ , as shown in Figure 3d. These faint spots appear to initially have a weak orientational correlation with the host  $\text{TiS}_2$  lattice, which diminishes with further heating and continued deintercalation. This observation suggests an in-plane partial-melting transition has occurred for regions of the Hg guest layers (e.g., layers, islands, or guest-edge dislocations). During the transition, regions of the Hg chains transform to have local lamellar hexagonal order resulting in the observed  $d$  spacings ( $2.70 \text{ \AA}$ ) for the locally close-packed Hg layers. The resulting inter-

(13) McKelvy, M. J.; Glaunsinger, W. S. *J. Solid State Chem.* **1987**, *66*, 181.

(14) Thompson, A. H.; Gamble, F. R.; Symon, C. R. *Mater. Res. Bull.* **1975**, *10*, 915.

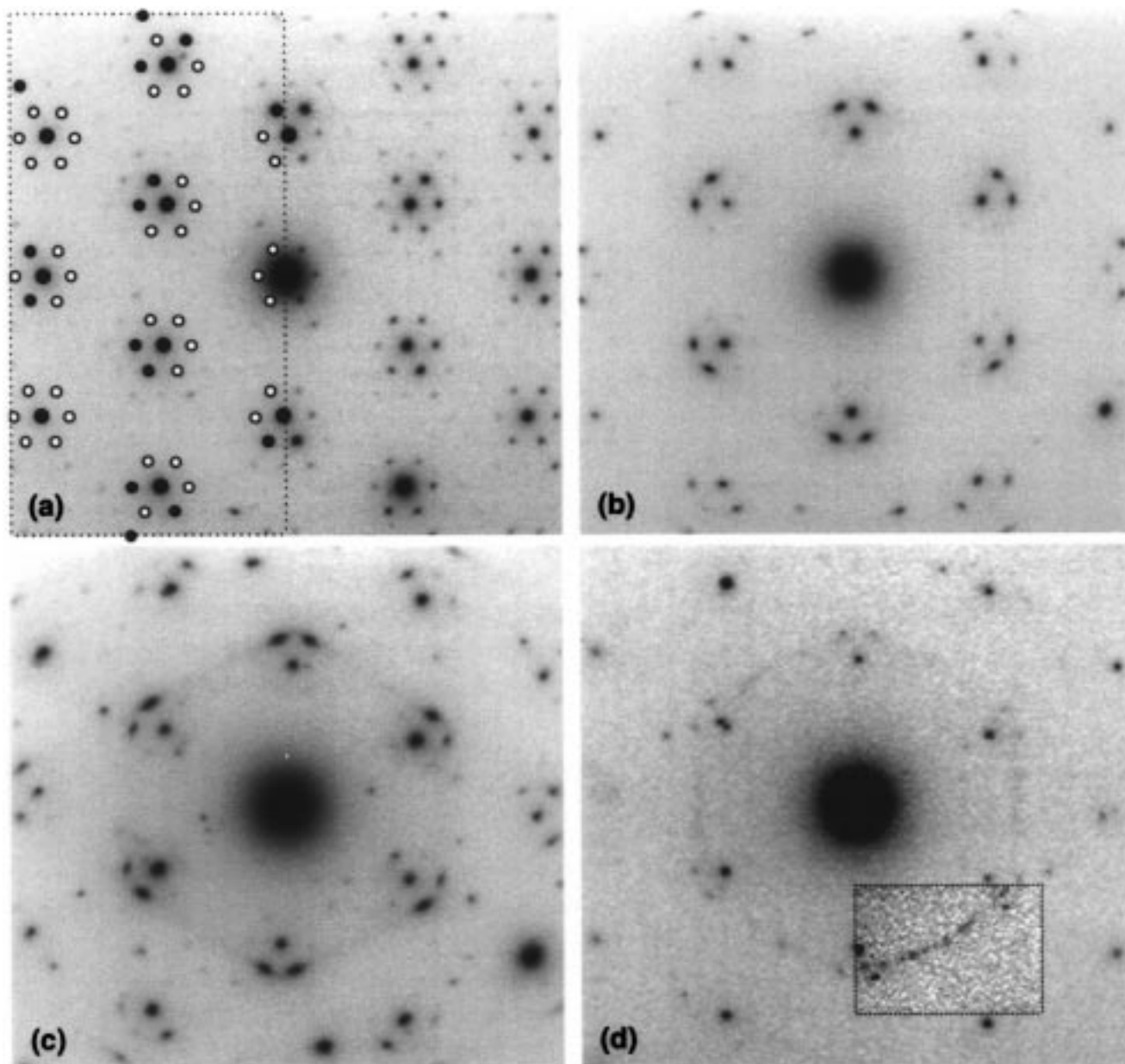


**Figure 3.**  $\text{Hg}_x\text{TiS}_2$  electron diffraction patterns as a function of increasing temperature and degree of deintercalation: (a) pattern taken at a substrate temperature of  $-170^\circ\text{C}$  with minimal deintercalation and electron-beam heating together with a schematic overlay (left) showing the primary  $\text{Hg}_x\text{TiS}_2$  reflections (black spots) and those arising from double diffraction (white spots in black outline); (b and c) patterns taken at progressively higher temperature showing increasing disorder along  $a^*$  and the absence of double diffraction; (d) pattern taken at a substrate temperature of  $50^\circ\text{C}$  together with sample beam-heating after substantial deintercalation; the inset is a contrast-enhanced region of the diffraction pattern showing the weak  $2.70\text{ \AA}$  reflections from the orientationally disordered, locally ordered hexagonal Hg layers and the residual weak  $\beta = 96^\circ$  Hg-sublattice reflections; the strongest remaining reflections correspond to the  $\text{TiS}_2$  sublattice.

atomic Hg–Hg distance of  $\sim 3.12\text{ \AA}$ , is close to that observed for liquid Hg ( $3.07\text{ \AA}$ ),<sup>15</sup> consistent with partial melting of the Hg guest layers to form regions with local lamellar hexagonal order.

The above observations suggest a general model for the structural behavior of  $\text{Hg}_x\text{TiS}_2$  as a function of temperature and level of deintercalation. First, at very low temperature the incommensurate Hg and  $\text{TiS}_2$  sublattices that comprise the  $\beta = 96^\circ$  structure are well-ordered, with few structural defects, as shown in Figure 1. Increasing temperature induces independent motion of the Hg chains along their chain-axis direction, result-

ing in increasing disorder and streaking along the  $a^*$  direction. Therefore, the interchain disorder previously observed at higher temperatures<sup>11</sup> is thermally induced, with the basic incommensurate  $\beta = 96^\circ$  structure being well-ordered at lower temperatures.

At higher temperatures, where deintercalation is prominent, the Hg chains undergo an intriguing partial-melting transition to form intercalant regions with local lamellar hexagonal order, as shown in Figure 4. These regions show weak and diminishing orientational correlation with the host-layer sublattice as a function of temperature. A melting transition has been observed by both XPD and DSC for the fully intercalated  $(\text{Hg}_{1.24}\text{TiS}_2)\beta = 102^\circ$  structure at similar temperatures

(15) Black, P. J. and Cundall, J. A. *Acta Crystallogr.* **1965**, *19*, 807.

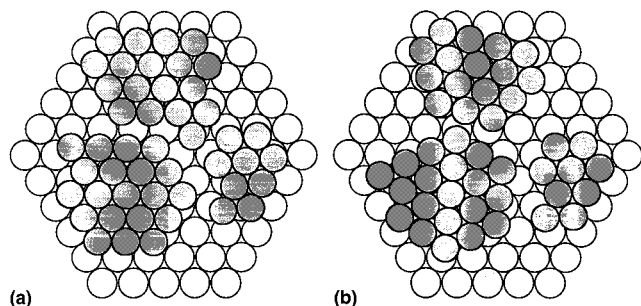


**Figure 4.** A schematic depiction of partially melted  $\text{Hg}_x\text{TiS}_2$  guest-layer regions, which exhibit local hexagonal order: (a) Hg regions with weak orientational correlation with the hexagonal  $\text{TiS}_2$  sublattice; (b) Hg guest-layer regions with little orientational correlation, likely to be found at higher temperature. The darker and lighter circles depict the Hg and S positions, respectively.

(200 °C, which is comparable to a substrate temperature of 50 °C combined with electron-beam heating).<sup>12</sup> However, above the transition temperature, all the unique Hg sublattice reflections for the fully intercalated material, which are sharp and well-defined, disappear. These reflections appear to be replaced by weak, broad, asymmetric lines, which suggest a heavily disordered stacking of the Hg layers. There was also a discontinuous increase (0.07 Å) in the interlamellar separation for these fully intercalated galleries at the transition, which may provide a two-dimensional freedom for the Hg guest layers facilitating the transition to a state with a low degree of lateral ordering of the guests.

In contrast, the partial-melting transition observed for the  $\beta = 96^\circ$  phase and the resulting local guest-layer

order may be associated with guest-island/edge dislocation formation during deintercalation.<sup>9,11</sup> These physical boundaries for the guest layers (especially guest islands) can restrict the amount of lamellar disorder in individual guest regions via the need for guest packing efficiency. Another factor that can contribute to the observed local order is the small increase ( $\sim 3\%$ ) in the two-dimensional packing area of the partially melted guest layers versus the  $\beta = 96^\circ$  guest layers. Since the transition actually forces guest islands/dislocations to expand by about 3%, they must push outward against their host-layer domain wall boundaries promoting guest-packing efficiency in the process.

This study has found that the host-layer boundaries that surround guest islands and dislocations not only can induce novel intercalate phase transitions by minimizing host-layer elastic strain,<sup>10,11</sup> but they can also substantially affect intragallery melting transitions, physically restraining the degree of guest-layer disorder.

**Acknowledgment.** We wish to acknowledge the National Science Foundation for support through grant DMR 91-06792 and acknowledgment is made to the donors of the Petroleum Research Fund, administered by the American Chemical Society, for partial support of this research. The synthesis and electron microscopy were conducted in the Center for Solid State Science's Goldwater Materials Science Laboratories at Arizona State University.

CM980437U